Trophoblast L-Selectin–Mediated Adhesion at the Maternal-Fetal Interface

Olga D. Genbacev,[1] Akraporn Prakobphol,[1] Russell A. Foulk,[4] Ana R. Krtolica,[5] Dusko Ilic,[1] Mark S. Singer,[2] Zhi-Qiang Yang,[6] Laura L. Kiessling,[6] Steven D. Rosen,[2] Susan J. Fisher[1,2,3]*

Trophoblast adhesion to the uterine wall is the requisite first step of implantation and, subsequently, placentation. At the maternal-fetal interface, we investigated the expression of selectin adhesion systems that enable leukocyte capture from the bloodstream. On the maternal side, human uterine epithelial cells up-regulated selectin oligosaccharide-based ligands during the window of receptivity. On the fetal side, human trophoblasts expressed L-selectin. This ligand-receptor system was functional, because beads coated with the selectin ligand 6-sulfo sLe^x bound to trophoblasts, and trophoblasts bound to ligand-expressing uterine luminal epithelium in tissue sections. These results suggest that trophoblast L-selectin mediates interactions with the uterus and that this adhesion mechanism may be critical to establishing human pregnancy.

Specialized mechanisms enable cell adhesion under flow. In the vasculature, interactions between leukocytes and endothelium are mediated by carbohydrate-binding proteins (selectins) that recognize specific oligosaccharide structures. These bonds have unusual properties that allow leukocyte capture through rolling adhesion from flowing blood (*1*). This initial step is rapidly followed by integrin activation, firm adhesion, and transmigration through the vessel wall into tissues (*1, 2*).

At the morphological level, there are parallels between leukocyte extravasation from the vasculature and attachment of the embryo/fetus to the uterine wall. In the latter instance, adhesion takes place under flow created by mucin secretion (*3*). Implantation begins with apposition: The free-floating blastocyst-stage embryo, which is captured by the uterine luminal epithelium, is easily dislodged (*4*). Shortly thereafter, the blastocyst firmly adheres to the uterine wall, and trophoblasts transmigrate across the luminal epithelium, burying the embryo beneath the uterine surface. Subsequent development depends on trophoblast adhesion under blood flow that is encountered as the cells breach uterine vessels, a process that diverts maternal blood to the placenta. At the molecular level, trophoblast adhesion from implantation onward is an integrin-dependent process (*5, 6*) that includes other mechanisms involved in leukocyte extravasation (*7*). Together, these parallels raised the possibility that the initial steps in implantation and placentation make use of other components of the leukocyte emigration system, such as selectins and their carbohydrate-based ligands.

To determine whether selectin ligands are present at appropriate times and locations to function in blastocyst adhesion to the uterus, we studied their expression at the maternal-fetal interface with antibodies that bind sulfated oligosaccharides that interact with L-selectin (*8*). We obtained endometrial biopsies from six donors during the follicular (nonreceptive) phase and serially during the luteal (receptive) phase. During the follicular phase, tissue sections of biopsy specimens stained weakly with MECA-79, an antibody that recognizes a sulfate and carbohydrate epitope on an important class of endothelial L-selectin ligands [dependent on $SO_3\rightarrow6$ *N*-acetylglucosamine (GlcNAc)] (*9*). Antibody reactivity localized to the surface of glandular and luminal epithelia (Fig. 1, A and B). However, during the luteal phase, the staining was much stronger, particularly on the luminal epithelium (Fig. 1, C and D). We stained the same samples with the HECA-452 antibody, which reacts with sLe^x (Siaα2→3Galβ1→4[Fucα1→3]GlcNAc) (Sia, sialic acid; Gal, galactose; Fuc, fucose) and related structures, including 6-sulfo sLe^x (Siaα2→3Galβ1→4[Fucα1→3][$SO_3\rightarrow6$]GlcNAc), 6′-sulfo sLe^x (Siaα2→3[$SO_3\rightarrow6$]Galβ1→4[Fucα1→3]GlcNAc), and 6′,6-disulfo sLe^x (Siaα2→3[$SO_3\rightarrow6$]Galβ1→4[Fucα1→3][$SO_3\rightarrow6$]GlcNAc) (*10*). In three donors, HECA-452 staining was also strongly up-regulated after ovulation (*11*). Staining with the PEN5 antibody, which recognizes a keratin sulfate–related lactosamine L-selectin ligand (*12*), increased along with MECA-79 immunoreactivity on uterine epithelium during the window of receptivity (compare Fig. 1, E and G) and shifted to decidual cells once pregnancy was established (Fig. 1I). Additionally, as

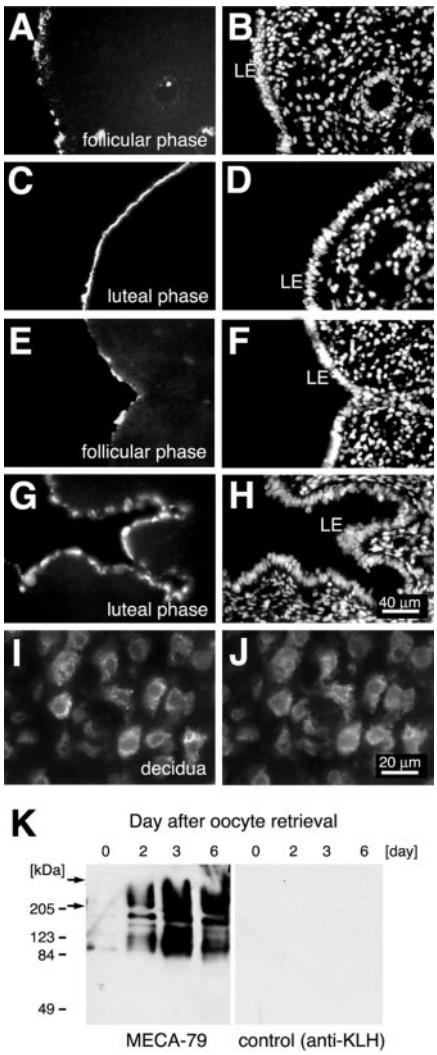

Fig. 1. Receptive human uterine epithelial cells express sulfated selectin oligosaccharide ligands in situ. Staining of uterine epithelia with MECA-79 (**A** and **C**) and PEN5 (**E** and **G**) was patchy and much less intense during the nonreceptive (follicular) phase of the cycle than during the receptive (luteal) phase. (**B**, **D**, **F**, and **H**) Hoechst staining. Only PEN5 (**I**) and antibody to prolactin (**J**) stained decidual cells of the pregnant uterus. (**K**) Immunoblot analyses (MECA-79) of endometrial biopsy samples taken from the same donor at oocyte retrieval (day 0) and 2, 3, and 6 days later confirmed the immunostaining results. LE, luminal epithelium.

Departments of [1]Stomatology, [2]Anatomy, and [3]Pharmaceutical Chemistry, University of California, San Francisco, CA 94143, USA. [4]Nevada Center for Reproductive Medicine, Reno, NV 89509, USA. [5]Life Sciences Division, Lawrence Berkeley National Laboratory, Berkeley, CA 94720, USA. [6]Departments of Chemistry and Biochemistry, University of Wisconsin, Madison, WI 53706, USA.

*To whom correspondence should be addressed. E-mail: sfisher@cgl.ucsf.edu

previously reported (*13*), uterine CD45$^+$ large granular leukocytes expressed this carbohydrate epitope (*11*). Analyses of samples later in gestation (*8*) showed that staining with MECA-79 and HECA-452 was lost during the second trimester, a situation that persisted until birth (*11*). PEN5 staining was retained on large granular leukocytes.

Immunoblot analyses (*8*) with MECA-79 confirmed up-regulation of selectin oligosaccharide ligands as the window of human receptivity opens (Fig. 1K). On day 0 (oocyte retrieval), we detected faint immunoreactive bands. On day 2, we observed stronger immunoreactivity in four areas—a diffuse, high molecular mass band(s) in the stacking gel and at least three bands in the 120- to 200-kD region of the running gel. The diffuse bands are expected for highly O-glycosylated proteins such as those that function as selectin ligands in high endothelial venules. The increase in MECA-79 reactivity on days 3 and 6 versus that on days 0 and 2 suggests that the concentration of selectin ligands increases as the uterus becomes receptive. The same patterns of MECA-79 reactivity were observed in samples obtained from a woman undergoing a natural cycle (*11*). We observed no immunoreactivity when we incubated a replica of the same lysates with an unrelated, rat isotype–matched control secondary antibody (antibody to keyhole limpet hemocyanin). Additional immunoblot analyses with HECA-452 and PEN5 showed that these antibodies primarily reacted with the very high molecular mass component(s) in the stacking gel (*11*). Together, these results suggest that expression of specific carbohydrate structures relevant to selectin recognition determinants is strongly up-regulated as the uterus becomes receptive. Whether marked alterations in glycosylation and sulfation track with changes in hormone levels in other tissues remains to be determined.

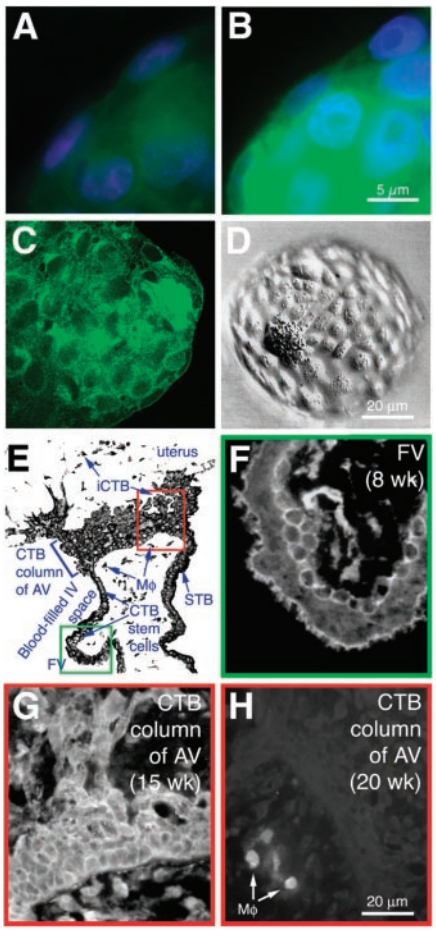

Fig. 2. Human trophoblasts express L-selectin in situ. (**A**) Before hatching, human trophectoderm showed little L-selectin staining (green, DREG-56; purple, Hoechst). (**B** and **C**) After hatching, the trophectoderm stained brightly for L-selectin. (**D**) Phase-contrast micrograph of (C). (**E**) Diagram of a placental anchoring villus (AV) attaching through a cytotrophoblast (CTB) column to the uterus and a floating villus (FV) in the blood-filled intervillous (IV) space. (**F** and **G**) Before 16 weeks, cytotrophoblasts, macrophages (Mϕ), and syncytiotrophoblasts (STBs) stained with DREG-56. (**H**) After 17 weeks, trophoblast staining was weak or absent, although macrophages retained strong antibody reactivity. iCTB, invasive cytotrophoblasts.

These findings prompted us to ask whether the trophectoderm of implantation-competent human embryos expresses L-selectin. Accordingly, we stained blastocysts, without permeabilization, with fluorescein isothiocyanate–conjugated antibody to L-selectin (*8*). Before the embryo hatched from the zona pellucida, L-selectin expression was either weak and diffuse or absent (Fig. 2A). After hatching, strong staining was observed in association with the trophectoderm (Fig. 2B) over the entire embryo surface (Fig. 2C), as indicated by phase-contrast microscopy (Fig. 2D).

Additionally, we analyzed L-selectin expression in tissue sections of the human maternal-fetal interface (*8*), which contained floating villi, so named because they float in maternal blood, and anchoring villi, which attach to the uterine wall (Fig. 2E). Anchoring villi contain trophoblasts in all stages of differentiation, including cytotrophoblast aggregates (cell columns) that span the blood-filled intervillous space to attach under shear stress to the uterine wall (Fig. 2E), where they intravasate maternal blood vessels (*11*). Between 6 and 16 weeks of gestation, cytotrophoblast progenitors (Fig. 2, F and G), cytotrophoblasts in cell columns, and invasive cytotrophoblasts (Fig. 2G) strongly reacted with an antibody that recognizes the L-selectin extracellular domain. The pattern of reactivity was indicative of antibody binding to cell-surface L-selectin. Overlying syncytiotrophoblasts, produced by cytotrophoblast fusion, also stained, as did macrophages in the villus stromal cores. To establish that trophoblast L-selectin staining was not due to adsorption of shed L-selectin from blood, we also used antibodies that recognized the carboxyl terminus of the molecule in immunolocalization experiments. The same populations of cells, with the exception of the syncytiotrophoblasts, stained with the L-selectin antibodies tested (*11*). However, from 17 weeks of gestation to term, there was reduced or no staining, although macrophages continued to react strongly (Fig. 2H). Because the selectins have overlapping functions in mediating leukocyte rolling adhesion, we examined human trophoblast expression of P- and E-selectin. Antibody to P-selectin inconsistently demonstrated weak staining of first- and second-trimester syncytiotrophoblasts, and antibody to E-selectin did not react with any of the samples (*11*).

To support our in situ observations, we characterized human trophoblast L-selectin expression in vitro (*8*) using two models of cytotrophoblast differentiation and uterine invasion. In an organ culture model, explanted anchoring villi are cultured on Matrigel-coated wells; villi attach via the remnants of severed cytotrophoblast columns, which then give rise to invasive cytotrophoblasts (*14*). Sections of explants cultured for 72 hours were stained with antibody to L-selectin. The pattern of antibody reactivity was very similar to that observed in situ; cytotrophoblast progenitors and invasive cytotrophoblasts stained, as did the syncytial surface (Fig. 3A). At higher magnification, the pattern of cytotrophoblast staining was indistinguishable from that of Jurkat cells that express L-selectin (*15*) (compare Fig. 3, B and C). In the second model, purified cytotrophoblast progenitors that are plated on Matrigel differentiate to invasive cells over 48 to 72 hours (*16*). After 48 hours, these cells also reacted with antibody to L-selectin (*11*). To confirm antigen identity, we analyzed lysates of isolated cytotrophoblasts and columns dissected from explants (*8*) (Fig. 3A) by immunoblotting samples that were separated on 10% polyacrylamide gels. Staining the blot with polyclonal antibody to human L-selectin revealed a broad 75- to 90-kD band (Fig. 3D). Jurkat and neutrophil lysates showed the same bands. Together, these data indicate that trophoblast up-regulation of L-selectin expression occurs concomitantly with attachment of blastocysts and, later, cytotrophoblasts to uterine epithelium.

We used two approaches to assess the functional state of trophoblast L-selectin in vitro. Under shear stress, beads (*8*) coated with 6-sulfo sLe^x (a recognition determinant for L-selectin) bound to chorionic villus explants (Fig. 3E). Beads bound to cytotrophoblast columns of anchoring villi and to the syncytiotrophoblast surface (that is, the cells that express L-selectin in situ and in vitro).

Beads that displayed sLe^x also bound to explants but in fewer numbers (*11*). This result is consistent with the finding that L-selectin binds more tightly to 6-sulfo sLe^x than to sLe^x (*2*). Few control phosphatidylcholine-conjugated beads bound to cytotrophoblast cell columns or syncytiotrophoblasts (Fig. 3F). Likewise, uncoated beads did not bind (*11*). Beads that displayed 6-sulfo sLe^x did not adhere to explants preincubated with an antibody that blocks L-selectin function (Fig. 3G), suggesting binding specificity.

We also compared cytotrophoblast and Jurkat adhesion to tissue sections cut from uterine biopsies, a method that allows visualization of leukocyte adhesion through L-selectin to lymph node high endothelial venules (*8, 17*) (Fig. 4, A to H). The data are quantified and summarized in Fig. 4I. Under shear stress, cytotrophoblasts, as single cells and clusters, primarily bound to the epithelial portion of the receptive (luteal phase) uterus, including the lumen (Fig. 4A). Adherent cells stained for L-selectin (Fig. 4B). Cytotrophoblasts also bound to glands and their contents (Fig. 4C). Adherence to both luminal (*11*) and glandular (Fig. 4D) epithelium was inhibited by adding antibody to L-selectin. Adherence was also inhibited when we preincubated the tissue sections with MECA-79 (Fig. 4I). Far fewer cytotrophoblasts bound to tissue sections of nonreceptive (follicular phase) biopsy specimens; epithelial adhesion was nearly absent (Fig. 4I). As a positive control, we tested Jurkat binding to tissue sections of luteal-phase uterine biopsies. The cells preferentially adhered to epithelia (for example, the luminal surface in Fig. 4E), and binding was inhibited by adding antibody to L-selectin (Fig. 4F) or MECA-79 (Fig. 4I). Like cytotrophoblasts, the cells often adhered to glands (Fig. 4G) that contained MECA-79–reactive secretions (Fig. 4H).

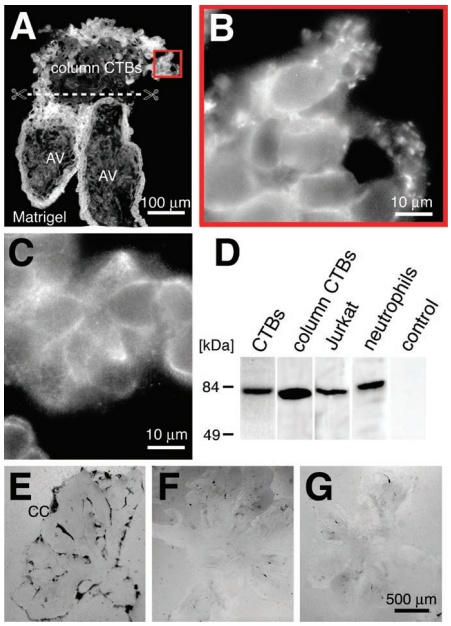

Fig. 3. Human trophoblasts express functional L-selectin in vitro. (**A**) The trophoblast layers of an anchoring villus (AV) explant and cytotrophoblasts that invaded the Matrigel (red box) stained with antibody to L-selectin (DREG-56). (**B**) Immunoreactivity was detected at cell surfaces and cell-cell contacts. (**C**) L-selectin–expressing Jurkat cells had a similar staining pattern. (**D**) Immunoblot analyses (antibody to CD62L) of lysates from purified cytotrophoblasts (CTBs), CTBs in columns dissected from cultured anchoring villi [scissors in (A)], Jurkat cells, and neutrophils revealed a single immunoreactive band that was absent when the primary antibody was omitted (control). (**E**) 6-Sulfo sLe^x–conjugated beads bound to trophoblasts covering anchoring villi. CC, cell columns. (**F**) Far fewer control (phosphatidylcholine-coated) beads attached. (**G**) Preincubating the villi with antibody to L-selectin (DREG-56) nearly abolished binding of 6-sulfo sLe^x–conjugated beads.

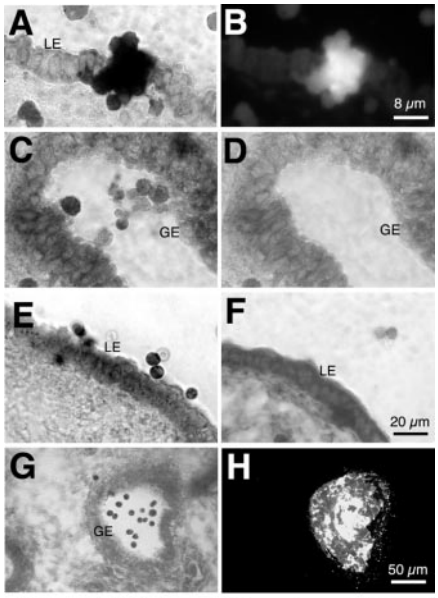

I

cells bound / phase / uterine cells	CTB luteal	CTB follicular	Jurkat luteal	Jurkat follicular
all cells	162 ± 43	39 ± 6	195 ± 36	19 ± 7
epithelia*	132 ± 35	4 ± 2	178 ± 47	4 ± 1
all cells + anti–L-selectin	29 ± 15	N.D.	30 ± 14	N.D.
epithelia + anti–L-selectin	0	N.D.	6 ± 3	N.D.
all cells + MECA-79	27 ± 15	N.D.	29 ± 15	N.D.
epithelia + MECA-79	3 ± 1	N.D.	5 ± 1	N.D.

Fig. 4. Human trophoblasts use L-selectin to bind uterine epithelial oligosaccharide ligands. (**A**) Cytotrophoblasts adhered to the luminal epithelium (LE) in tissue sections of human luteal-phase endometrial biopsies. (**B**) Adherent cells stained for L-selectin. Cytotrophoblast binding to glandular epithelium (GE) (**C**) was inhibited with antibody to L-selectin (**D**). Binding of L-selectin–expressing Jurkat cells to luteal-phase luminal epithelium (**E**) was inhibited by antibody to L-selectin (**F**). Jurkat cells also bound to glands (**G**) that contained MECA-79–reactive secretions (**H**). (**I**) Summary of experiments and quantification of binding. *Luminal and glandular epithelium, glandular secretions. Values are expressed as means ± SD. N.D., not determined.

Our finding led us to question why mice without L-selectin reproduce (*18*). We immunostained implantation-competent mouse blastocysts for L-selectin and receptive murine uteri for its ligands (*8, 11*). Mouse trophectoderm expressed cell-surface L-selectin. Receptive murine uterine luminal and glandular epithelium stained with HECA-452, which reacts with carbohydrate epitopes, but not with MECA-79, which requires sulfation for binding. The latter observation suggests that the sulfated carbohydrate structures that are the major L-selectin ligands in lymph nodes and receptive uterus (Fig. 1, C and K, and Fig. 4I) are absent at the time of murine implantation.

Our finding of L-selectin functions outside the blood-vascular system has several important implications for implantation and placentation. Shear stress, required for optimal L-selectin–mediated adhesion in the vasculature, is likely an important component of both processes. Given the many and varied causes of infertility and early pregnancy loss, defects in the selectin adhesion system could account for a portion of unexplained reproductive failures, as well as deficient cytotrophoblast invasion, which is associated with pregnancy complications such as preeclampsia (*19*). Our data also provide further insights into the highly unusual nature of trophoblasts. Previously, we showed that invasive cytotrophoblasts of ectodermal origin undergo a novel differentiation process, taking on characteristics of vascular cells (*5*). Our finding that these cells also share leukocyte adhesion mechanisms suggests that trophoblasts have characteristics of the hemangioblast stem cell population that gives rise to both blood cells and vessels. Whether this unusual phenotype is related to the observation that implantation is an inflammatory-like process remains to be determined (*20*). The implications include the possibility that interactions between L-selectin–bearing trophoblasts and PEN5-positive decidual natural killer cells could help target this unusual population of immune cells to the uterus. Together, our results suggest close links, at the molecular level, between processes that are key to reproductive, immune, and vascular functions.

References and Notes

1. R. Alon, S. Feigelson, *Semin. Immunol.* **14**, 93 (2002).
2. R. P. McEver, *Curr. Opin. Cell Biol.* **14**, 581 (2002).
3. R. R. Isberg, P. Barnes, *Cell* **110,** 1 (2002).
4. E. R. Norwitz, D. J. Schust, S. J. Fisher, *N. Engl. J. Med.* **345**, 1400 (2001).
5. C. H. Damsky, S. J. Fisher, *Curr. Opin. Cell Biol.* **10**, 660 (1998).
6. D. Ilic *et al.*, *Am. J. Pathol.* **159**, 93 (2001).

7. P. M. Drake *et al*., *J. Exp. Med.* **193**, 1199 (2001).
8. Materials and methods are available as supporting material on *Science* Online.
9. J. C. Yeh *et al*., *Cell* **105**, 957 (2001).
10. C. Mitsuoka *et al*., *Biochem. Biophys. Res. Commun.* **230**, 546 (1997).
11. O. D. Genbacev *et al*., data not shown.
12. P. Andre *et al*., *Proc. Natl. Acad. Sci. U.S.A.* **97**, 3400 (2000).
13. S. Calatayud *et al*., *Int. Immunol.* **8**, 1637 (1996).
14. O. Genbacev *et al*., *Placenta* **13**, 439 (1992).
15. P. A. Giblin *et al*., *J. Immunol.* **159**, 3498 (1997).
16. C. L. Librach *et al*., *J. Cell Biol.* **113**, 437 (1991).
17. H. B. Stamper Jr., J. J. Woodruff, *J. Exp. Med.* **144**, 828 (1976).
18. P. S. Frenette, D. D. Wagner, *Thromb. Haemost.* **78**, 60 (1997).
19. Y. Zhou *et al*., *J. Clin. Invest.* **99**, 2152 (1997).
20. S. J. Kimber, C. Spanswick, *Semin. Cell Dev. Biol.* **11**, 77 (2000).
21. Supported by NIH grants DE 07244, HL 64597, and U01 HD 42283 (part of the Cooperative Program on Trophoblast-Maternal Tissue Interactions) (S.J.F.) and NIGMS R37GM23547 (S.D.R.). We thank M. McKenney and E. Leash for excellent editorial advice.

Supporting Online Material
www.sciencemag.org/cgi/content/full/299/5605/405/DC1
Materials and Methods
References

18 October 2002; accepted 26 November 2002

Endoproteolytic Activity of the Proteasome

Chang-Wei Liu, Michael J. Corboy, George N. DeMartino,* Philip J. Thomas*

The proteasome plays a central role in the degradation of regulatory and misfolded proteins. Current models suggest that substrates access the internal catalytic sites by processively threading their termini through the gated substrate channel. Here, we found that latent (closed) and activated (open) proteasomes degraded two natively disordered substrates at internal peptide bonds even when they lacked accessible termini, suggesting that these substrates themselves promoted gating of the proteasome. This endoproteolysis provides a molecular mechanism for regulated release of transcription factors from inactive precursors as well as a means of accessing internal folding defects of misfolded multidomain proteins.

The proteasome degrades the majority of cellular proteins in eukaryotes. Its activity allows for surveillance by the immune system, controls the levels of various regulatory proteins, and prevents the accumulation of misfolded mutant and damaged proteins (*1*). The architecture of the proteasome occludes its active sites within the lumen of a cylinder formed by four heptameric rings (*2*, *3*). This arrangement prevents well-folded proteins from entering the constricted annulus, protecting them from degradation, and has led to a model by which unfolded substrates are fed from their termini into the central catalytic cavity as extended chains and are degraded processively (*4*, *5*). However, this model cannot account for the proteasome-dependent release of active transcription factor domains from inactive precursors by partial degradation (*6*–*8*). For example, the p50 subunit of nuclear factor κ B transcription factor is produced by proteasome-dependent cotranslational processing of p105 (*6*). Because p50 constitutes the NH_2-terminus of p105 and the COOH-terminus is presumably blocked by the ribosome, the proteasome must either wait for release of nascent p105 from the ribosome or activate another protease that catalyzes the initial endoproteolytic step, as in the proteasome-dependent activation of Esp1 protease during sister chromatid exchange (*9*). Alternatively, the proteasome itself could enter ribosomally bound p105 at an internal site and initiate processing with an endoproteolytic cleavage.

To determine whether proteasome-mediated degradation is initiated from an internal site of a protein, we used two physiological substrates: the cyclin-dependent kinase (CDK) inhibitor $p21^{cip1}$ (p21) and α-synuclein (α-syn). Both proteins are "natively disordered" (*10*) and are efficiently degraded by the proteasome in the absence of polyubiquitin modification (*11*, *12*). We compared the degradation of these unstable substrates by the latent 20S proteasome (*13*) with that of the activated, assembled 26S particle (*14*). The 26S particle, the accepted physiological form of the proteasome, is composed of the 20S core particle and the PA700 (19S) regulatory cap (*14*). PA700 contains polyubiquitin (*15*, *16*) and misfolded protein (*17*, *18*) binding sites, isopeptidase activity (*19*, *20*), and adenosine triphosphatase subunits presumably involved in unfolding substrates (*21*). Both the 20S and 26S proteasomes efficiently degraded p21 and α-syn (Fig. 1A) (*22*). In contrast, the hyperstable green fluorescent protein (GFP) (melting temperature, T_m, > 65°C) (*23*) was not degraded by either 20S or 26S (Fig. 1B). The disordered substrates were efficiently degraded by the latent 20S proteasome despite its inability to hydrolyze short peptide substrates (Fig. 1C). Thus, unfolded proteins could open the "gate" that controls access to the otherwise occluded catalytic sites, thereby initiating a process similar to that employed by the proteasome regulators PA700 (*24*) and PA28 (*25*).

When fusions between the unfolded substrates and the stable GFP were assessed, both the latent 20S and the active 26S proteasomes efficiently degraded the p21 and α-syn domains but not the GFP domain of each fusion protein (Fig. 2, A and B), suggesting that additional factors were required for efficient unfolding of this stable domain. We also examined whether either the 20S or the 26S proteasome exhibited a directional preference by comparing the degradation of fusion proteins that contained GFP at either the NH_2- or COOH-terminus (Fig. 2C). The relative activities of the 20S and 26S proteasomes were equivalent toward the p21 fusions. For the α-syn fusions, the 20S proteasome degraded the substrates faster, although the 26S reaction did go to completion (inset, Fig. 2B). Apparently, the shorter α-syn, when blocked with GFP, was less accessible to the longer channel of the 26S proteasome. In this regard, the 26S and 20S proteasomes exhibited similar activity toward unprotected α-syn (Fig. 1A) and circular α-syn whose termini were blocked by a peptide bond. For all substrates, degradation was effectively inhibited by MG132 (Fig. 2C), a potent proteasome inhibitor. Finally, the proteasome degraded the substrates blocked at either terminus at equivalent rates (Fig. 2C), indicating that the reported preference for COOH- to NH_2-terminal degradation (*4*) is not a general feature of all substrates.

To assess the ability of the proteasome to cleave these substrates at internal sites, we protected both termini of p21 and α-syn by sandwiching them between nondegradable GFP domains (Fig. 3). As assessed by immunoblotting, GFP-p21-GFP and GFP–α-syn–GFP proteins were degraded by the 20S and 26S proteasomes, and degradation was inhibited by MG132. The rate of degradation of bilaterally protected substrates was slower than the degradation of p21 alone, α-syn alone (Fig. 1A), and substrates protected at a single terminus (Fig. 2C), indicating that the endoproteolytic cleavage was less efficient than degradation from the termini. Again, neither GFP-blocking domain

Department of Physiology, University of Texas Southwestern Medical Center at Dallas, Dallas, TX 75390, USA.

*To whom correspondence should be addressed. E-mail: philip.thomas@utsouthwestern.edu (P.J.T.); george.demartino@utsouthwestern.edu (G.N.D.)